Estimating the process noise variance for vehicle motion models

Jan Erik Stellet[1], Fabian Straub[2], Jan Schumacher[1], Wolfgang Branz[1], J. Marius Zöllner[3]

***Abstract*— Vehicle motion models are employed in driver assistance systems for tracking and prediction tasks. For probabilistic decision making and uncertainty propagation, the prediction's inaccuracy is taken into account in the form of process noise. This work estimates Gaussian process noise models from measured vehicle trajectories using the expectation maximisation (EM) algorithm. The method is exemplified and the results evaluated for three commonly used motion models based on a large-scale dataset. A novel closed-form adaptation of the algorithm to a covariance matrix with Kronecker product structure, as in models for translational motion, is presented. The findings suggest that the longitudinal prediction errors feature a non-Gaussian distribution but a reasonable approximation is given by the estimated model.**

I. Introduction

A. Motivation

Situation analysis for driver assistance functions requires predicting the behaviour of traffic participants in the next few seconds. Due to an incomplete and uncertain perception of the environment, predictions are affected by uncertainty, see Fig. 1. Probabilistic uncertainty models are hence crucial for the design of sensors and decision making [1].

Besides the obvious cause of noisy sensor measurements, the future behaviour of traffic participants is never certain. Thus, modelling the uncertainty which is introduced by inaccurate prediction models is necessary, which is the scope of this work. Subsequently, the two sources of uncertainty can be propagated to decision making algorithms, i.e. criticality measures for collision avoidance systems, which has been discussed in our previous contribution [2].

Valuable insight is obtained from models that can be analytically propagated, e.g. Gaussian distributions. This choice requires compromises in the achievable modelling accuracy but yields the benefit of understanding the general case, whereas numerical propagation allows singular evaluations for initial state and parameter values only [3].

Therefore, this work employs the expectation maximisation (EM) algorithm to estimate the parameters of Gaussian vehicle motion models using a large-scale dataset of vehicle trajectories ($\approx$ 170 h of raw recordings). With a disjoint dataset for evaluation, the predictions are evaluated in terms of accuracy as well as congruence between the Gaussian uncertainty model and the empirical error distribution for a prediction horizon of up to $t_{\mathrm{pred}} = 3\,\mathrm{s}$.

[1]Jan Erik Stellet, Jan Schumacher and Wolfgang Branz are with Robert Bosch GmbH, Corporate Research, Vehicle Safety and Assistance Systems, 71272 Renningen, Germany

[2]Fabian Straub is with Robert Bosch GmbH, Gasoline Systems, Engineering SW Basesystem, 70469 Stuttgart, Germany

[3]J. Marius Zöllner is with Research Center for Information Technology (FZI), 76131 Karlsruhe, Germany

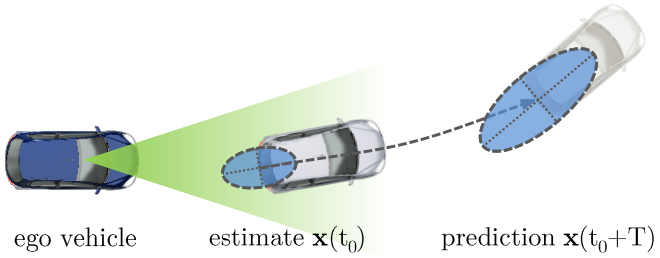

Fig. 1: Using environment perception sensors, the observed vehicle's current motion is estimated and its future course predicted. Uncertainty in the prediction arises from uncertain estimates of the initial state and model deviations, i.e. process noise. This work identifies Gaussian process noise models.

B. Related work

Prediction models have two main applications in the driver assistance context, namely in object tracking and situation interpretation. Hence, related works on *evaluation* and *parameter estimation* for these models are reported in both areas. The difference is the time-span over which a prediction is made, that is either a fraction of a second for the system sampling time or multiple seconds for situation analysis.

For object tracking, e.g. using a Kalman filter, a number of motion models with white Gaussian process noise are known [4]. In order to make a sensible choice, the overall accuracy of the tracking filter results can be evaluated. This is done either in simulations [5] or based on real-world trajectories [6]. For a meaningful evaluation of probabilistic models, not only the accuracy of the mean trajectory but also the reliability of the predicted uncertainty is studied here.

Concerning the choice of the process noise covariance, two approaches can be differentiated. Either, the variance is selected as an upper expected deviation between the model and a true trajectory. When modelling vehicle behaviour, bounds can be derived from the maximum acceleration capabilities [7], [8]. In a tracking algorithm, such a conservative choice minimises the risk of a track loss. For long-term predictions though, large and barely conclusive covariance predictions are a consequence because any physically possible trajectory is enclosed. Alternatively, the expectation maximisation principle can be used for an on-line estimation [9], [10].

Concerning prediction models for situation assessment, a plethora of works exist on the design, parameter inference and evaluation [11]. For example, [12] proposes a sophisticated Markovian model which incorporates multiple semantic aspects such as intentions and interactions.

The focus of this contribution, though, is on uncertainty propagation in a given function where simple, purely kinematic models are implicitly assumed. For example, common criticality measures are currently based on the constant

 DOI 10.1109/ITSC.2015.212

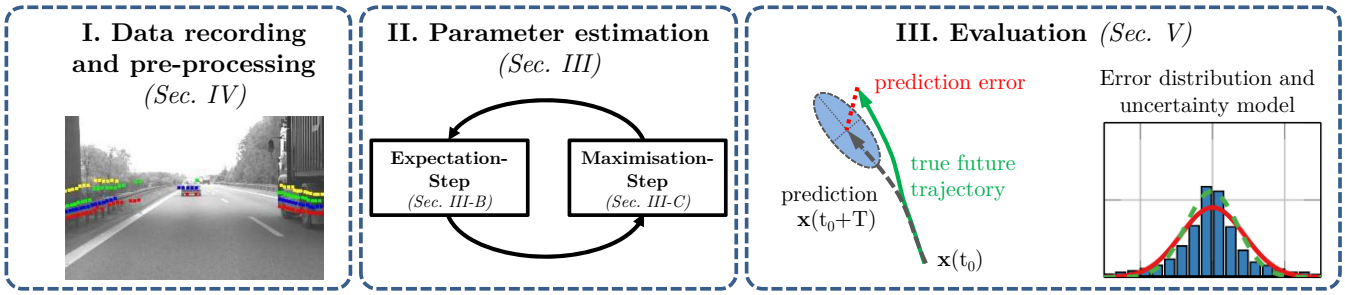

Fig. 2: The process noise covariance is estimated using the expectation maximisation algorithm, which is first introduced in Sec. III and subsequently applied to our dataset in Sec. IV. The results are evaluated by comparing the empirical distribution of the prediction errors to the obtained analytical uncertainty model in Sec. V.

acceleration (CA) model [13]. Deriving criticality algorithms from more advanced models can improve the results [14], which is however not the scope of this work.

From a methodological point of view, using the expectation maximisation principle [15] for model identification of stochastic dynamic systems is known in many fields, e.g. in the robotics domain [16], [17]. Concerning vehicle motion models, similar analyses have to the best of the authors' knowledge not been reported.

The scope of this work should not be confused though with models of the car-following behaviour as used in microscopic traffic simulations. There is a significant body of works on model identification using naturalistic driving data, e.g. [18], but these models concern the interactions of a driver with a preceding vehicle. For a driver assistance system, this information is however usually unknown as vehicles in front of the observed one are occluded.

C. Contributions and outline

This work is organised as outlined in Fig. 2. The main contribution is a data-driven approach for estimating Gaussian process noise parameters for vehicle motion models as is described in the problem formulation in Sec. II. Sec. III comprises an introduction of the employed expectation maximisation algorithm. A novel theoretical contribution presented in Sec. III-D is a closed-form adaptation of the algorithm to a process noise covariance matrix given by a Kronecker product with one known and unknown factor. This structure arises in linear translational models, e.g. the constant acceleration model.

Applying the EM-algorithm to large datasets may become computationally and numerically challenging. Sec. IV-A discusses these aspects and compiles advice for practitioners on commonly experienced issues. In order to carry out the estimation on our set of vehicle trajectories measured by exteroceptive sensors, several pre-processing steps are first performed. Together with details on the employed dataset, these are detailed in Sec. IV-B.

The assumption of Gaussian white noise processes is commonly favoured in order to achieve simple, closed-form solutions. A contribution of the evaluation in Sec. V is to critically study the model's validity using a large-scale dataset of real-world trajectories.

II. Problem Formulation

A. Model representation

A n-dimensional state vector $\mathbf{x}(t) \in \mathbb{R}^n$ describes the kinematic motion state, e.g. position, velocities, acceleration. The motion dynamics are then given by a non-linear differential equation $\dot{\mathbf{x}}(t) = \mathbf{f}(\mathbf{x}(t))$.

Given an initial state $\mathbf{x}(t_0)$, one can solve the differential equation and obtain a prediction $\mathbf{x}(t_0 + T)$ as [19]:

$$\mathbf{x}(t_0 + T) = \mathbf{\Phi}(t_0 + T, t_0)\,\mathbf{x}(t_0)\,, \tag{1a}$$

$$\mathbf{\Phi}(t, t_0) = \exp\left(\int_{t_0}^{t} \mathbf{F}(\tau)\,\mathrm{d}\tau\right),\ \mathbf{F}(t) := \nabla_{\mathbf{x}(t)}\mathbf{f}(\mathbf{x}(t))\ . \tag{1b}$$

Concerning the accuracy of this prediction, two kinds of deviations can be differentiated [11]:

- *Manoeuvre changes:* Abrupt changes in the driven manoeuvre, e.g. from straight driving to turning, can occur. This may be expressed as an unknown, deterministic input signal $\mathbf{u}(t)$ in $\dot{\mathbf{x}}(t) = \mathbf{f}(\mathbf{x}(t), \mathbf{u}(t))$.
  As these changes are not included in the previous motion state $\mathbf{x}(t)$ they can only be inferred on a higher level of abstraction than the kinematic quantities, e.g. from context information or driver intention estimation.
- *Stochastic disturbances:* The focus of this work is on small perturbations that occur during the same driven manoeuvre. For example, while driving along a straight road the vehicle's velocity can vary due to slopes.
  It is hence assumed that no manoeuvre changes occur during the considered prediction horizon. This assumption is derived from the overall scope of our work which is on collision avoidance systems for situations with a high risk of an imminent collision. Thus, only short-time predictions are considered with a prediction horizon of up to 3 s.

The stochastic disturbances are modelled as additive white Gaussian process noise $\mathbf{w}(t) \in \mathbb{R}^{n_S}$ with time-invariant power spectral density $\mathbf{S}$ and $\mathbf{L} \in \mathbb{R}^{n \times n_S}$:

$$\begin{aligned} \dot{\mathbf{x}}(t) &= \mathbf{f}(\mathbf{x}(t)) + \mathbf{L}\mathbf{w}(t)\,, \\ \mathbb{E}\left[\mathbf{w}(t)\,\mathbf{w}(t')^{\top}\right] &= \mathbf{S}\delta(t - t')\ . \end{aligned} \tag{2}$$

If $\mathbf{S}$ and a Gaussian estimate $\hat{\mathbf{x}}(t_0) \sim \mathcal{N}(\mathbf{x}(t_0), \mathbf{\Sigma}_\mathbf{x}(t_0))$ with mean $\mathbf{x}(t_0)$ and covariance $\mathbf{\Sigma}_\mathbf{x}(t_0)$ are known, the covariance of the state prediction $\mathbf{\Sigma}_\mathbf{x}(t_0+T)$ is given to first order as [19]:

$$\mathbf{\Sigma}_\mathbf{x}(t_0+T) = \mathbf{\Phi}(t_0+T,t_0)\,\mathbf{\Sigma}_\mathbf{x}(t_0)\,\mathbf{\Phi}^\top(t_0+T,t_0) + \mathbf{Q}(t_0+T,t_0), \tag{3a}$$

$$\mathbf{Q}(t,t_0) = \int_{t_0}^{t} \mathbf{\Phi}(t,\tau)\,\mathbf{L}\mathbf{S}\mathbf{L}^\top\mathbf{\Phi}^\top(t,\tau)\,\mathrm{d}\tau\,. \tag{3b}$$

Therefore, the goal of this work can be summarised as estimating $\mathbf{S}$ from recorded measurement data.

However, measurement data is obtained by sampling at discrete points in time, hence we additionally have to introduce the discrete-time equivalent of (2). We assume a constant sampling time T and denote $t_k = k \cdot T$, $\mathbf{x}_k := \mathbf{x}(t_k)$, $\mathbf{f}(\mathbf{x}_k) := \mathbf{\Phi}(t_{k+1},t_k)\,\mathbf{x}(t_k)$ and $\mathbf{Q}_k := \mathbf{Q}(t_{k+1},t_k)$:

$$\mathbf{x}_{k+1} = \mathbf{f}(\mathbf{x}_k) + \mathbf{w}_k,\ \mathrm{cov}(\mathbf{w}_k) = \mathbf{Q}_k\,. \tag{4}$$

In general, $\mathbf{Q}_k$ now depends on the sampling time T, the spectral density $\mathbf{S}$ and the state $\mathbf{x}_k$ due to (1b). For the important special case of linear dynamics $\dot{\mathbf{x}}(t) = \mathbf{F}\mathbf{x}(t)$, the latter dependence vanishes and $\mathbf{Q}$ becomes time-invariant.

Note that the derivation of $\mathbf{Q}_k$ using (3b) assumes that a continuous-time noise process is sampled. Alternatively, discrete-time noise inputs can be directly modelled, assuming a constant amplitude and covariance $\mathbf{Q}_k$ between two sampling time instants [4], [20], [21]. This is a viable approach if solely the discrete-time system is considered, e.g. in a tracking filter, but not applicable to our case as the link to the continuous-time prediction (3) is lost.

Moreover, five different representations are known for the transformation from continuous to discrete time in non-linear models [20]. The approach followed in this work is termed discretised linearisation which is also employed in [3]. This choice is supported by consistency to linear systems, where the same equations are found as the exact propagation [19].

Lastly, the available measurement data usually comprises a partial and uncertain representation $\mathbf{y}_k \in \mathbb{R}^m$ of the state only. This is expressed by a non-linear measurement function $\mathbf{h}(\cdot)$ and additive white Gaussian noise $\mathbf{v}_k \sim \mathcal{N}(\mathbf{0}, \mathbf{R}_k)$:

$$\mathbf{y}_k = \mathbf{h}(\mathbf{x}_k) + \mathbf{v}_k\,. \tag{5}$$

In this work, 2-D range measurements from a laser scanner are used. Therefore, the measurements are formed by a linear mapping $\mathbf{h}(\mathbf{x}_k) = \mathbf{C}\mathbf{x}_k$ from the state vector $\mathbf{x}_k$, where only the Cartesian position is included in $\mathbf{y}_k$ ($m = 2$).

B. Kinematic motion models

Motion models that are frequently used in ADAS applications [6] can be differentiated by their level of complexity:

- In terms of the order of time differentials which are comprised in the state vector, e.g. velocity, acceleration, jerk etc. Considering higher derivatives leads to more unknown state variables. At the cost of increased state estimation effort, higher fidelity is possible. Furthermore, either a Cartesian or polar representation of velocity and acceleration may be beneficial [21].
- In terms of the dynamics: Models either assume purely translational motion or take an additional rotation into account (curvilinear models). The advantage of the former is their linearity, at the cost of realism. Hence, closed-form expressions for the exact estimation and prediction of Gaussian states can be employed.

The differential equations of three commonly used models, the linear constant velocity (CV) and constant acceleration (CA) as well as the non-linear constant turn rate and acceleration (CTRA) model are summarised in Tab. I.

In general, it might be impossible to find closed-form solutions for the state and uncertainty propagation from (1)-(3). Fortunately, these models make well-known exceptions and we refer to [3] and [6] for details.

C. Estimation of process noise parameters

If a time-series of the true states $\mathbf{x}_k$ was known, one could solve (4) for $\mathbf{w}_k = \mathbf{x}_{k+1} - \mathbf{f}(\mathbf{x}_k)$ and obtain a covariance estimate. In practice though, the estimation must be conducted using noisy measurements $\mathbf{y}_k$. We assume that $e = 1, \ldots, N_\mathrm{seq}$ independent series with $k = 1 \ldots N$ samples each are available and denote these as $\mathbf{Y} := \left\{\mathbf{y}_k^{(e)}\right\}$.[1]

Then, the stochastic system (4) and measurement model (5) can be used to formulate the probability density function $p(\mathbf{Y}|\boldsymbol{\theta})$ of these measurement series. This density depends on the unknown parameter $\boldsymbol{\theta}$, which e.g., defines the process noise covariance.

According to the maximum likelihood principle, maximising the log-likelihood $l_\mathbf{Y}(\boldsymbol{\theta}) := \log p(\mathbf{Y}|\boldsymbol{\theta})$ yields the most likely parameter estimate that explains the observations:

$$\hat{\boldsymbol{\theta}} = \arg\max_{\boldsymbol{\theta}} l_\mathbf{Y}(\boldsymbol{\theta})\,. \tag{6}$$

However, this maximisation becomes very difficult in practice. An efficient, iterative approach is the EM-algorithm [15] and will be introduced in the following section.

In [22], pedestrian dynamics are modelled and as an alternative estimation method, Bayesian inference is favoured over the maximum likelihood approach in order to avoid overfitting. Extensive training and evaluation datasets will be employed here to cope with this issue.

III. Expectation maximisation algorithm for process noise covariance estimation

A. The EM-principle

The central idea is to reformulate $l_\mathbf{Y}(\boldsymbol{\theta})$ using the states $\mathbf{X} := \left\{\mathbf{x}_k^{(e)}\right\}$ as $l_{\mathbf{Y},\mathbf{X}}(\boldsymbol{\theta}) = \log p(\mathbf{Y},\mathbf{X}|\boldsymbol{\theta})$. Since $\mathbf{X}$ is unknown, the complete log-likelihood is unavailable. But, given an estimate $\hat{\boldsymbol{\theta}}_l$, one can estimate the distribution of $\mathbf{X}$ and find the expected log-likelihood (E-Step):

$$q_{\hat{\boldsymbol{\theta}}_l}(\boldsymbol{\theta}) = \mathbb{E}\left[\log p(\mathbf{Y},\mathbf{X}|\boldsymbol{\theta})\right]\,. \tag{7}$$

[1] For notational convenience, it is assumed that the measurement time-series are of equal length N. This is however not a restriction and the method can be similarly derived for individual lengths N_e, $e = 1, \ldots, N_\mathrm{seq}$.

TABLE I: Motion model differential equations.

Constant velocity (CV)	**Constant acceleration (CA)**	**Constant turn rate and acceleration (CTRA)**
$\begin{bmatrix} \dot{x}(t) \\ \dot{v}_x(t) \\ \dot{y}(t) \\ \dot{v}_y(t) \end{bmatrix} = \begin{bmatrix} v_x(t) \\ 0 \\ v_y(t) \\ 0 \end{bmatrix} + \begin{bmatrix} 0 & 0 \\ 1 & 0 \\ 0 & 0 \\ 0 & 1 \end{bmatrix} \begin{bmatrix} w_x(t) \\ w_y(t) \end{bmatrix}$	$\begin{bmatrix} \dot{x}(t) \\ \dot{v}_x(t) \\ \dot{a}_x(t) \\ \dot{y}(t) \\ \dot{v}_y(t) \\ \dot{a}_y(t) \end{bmatrix} = \begin{bmatrix} v_x(t) \\ a_x(t) \\ 0 \\ v_y(t) \\ a_y(t) \\ 0 \end{bmatrix} + \begin{bmatrix} 0 & 0 \\ 0 & 0 \\ 1 & 0 \\ 0 & 0 \\ 0 & 0 \\ 0 & 1 \end{bmatrix} \begin{bmatrix} w_x(t) \\ w_y(t) \end{bmatrix}$	$\begin{bmatrix} \dot{x}(t) \\ \dot{y}(t) \\ \dot{v}(t) \\ \dot{\theta}(t) \\ \dot{a}(t) \\ \dot{\omega}(t) \end{bmatrix} = \begin{bmatrix} v(t)\cos(\theta(t)) \\ v(t)\sin(\theta(t)) \\ a(t) \\ \omega(t) \\ 0 \\ 0 \end{bmatrix} + \begin{bmatrix} 0 & 0 \\ 0 & 0 \\ 0 & 0 \\ 0 & 0 \\ 1 & 0 \\ 0 & 1 \end{bmatrix} \begin{bmatrix} w_a(t) \\ w_\omega(t) \end{bmatrix}$

Instead of maximising $l_{\mathbf{Y},\mathbf{X}}(\boldsymbol{\theta})$, a new estimate $\hat{\boldsymbol{\theta}}_{l+1}$ is thus obtained from $q_{\hat{\boldsymbol{\theta}}_l}(\boldsymbol{\theta})$ (M-Step):

$$\hat{\boldsymbol{\theta}}_{l+1} = \arg\max_{\boldsymbol{\theta}} q_{\hat{\boldsymbol{\theta}}_l}(\boldsymbol{\theta}) \ . \tag{8}$$

It can be shown that this iterative procedure of approximating the unknown log-likelihood and refining the result with a new estimate converges to the maximum likelihood estimate (6) [15]. As convergence criterion, the difference in the log-likelihood values from two subsequent iterations can be compared to a threshold value $\Delta q_{\min}$.

One remarkable property is that both steps of the algorithm can be efficiently performed for the (non-) linear Gaussian systems that are considered here. The following outline is a brief summary of the derivations found, e.g. in [16], [23].

B. E-Step

The goal is to firstly estimate the distribution $p(\mathbf{X})$ from $\mathbf{Y}$ and then calculate the expectation (7).

Provided that an estimate of $\hat{\mathbf{Q}}_l$ is known, the Extended Kalman smoother (EKS) algorithm can be applied to obtain a Gaussian estimate of the joint densities $p\left(\mathbf{x}_k^{(e)}, \mathbf{x}_{k-1}^{(e)}\right)$, $k = 2, \ldots, N$ for each time-series. Due to the Markovian assumption, this is a full description of $p(\mathbf{X})$. Basically, the EKS is a generalisation of the Extended Kalman filter to the full measurement sequence in order to obtain the estimate $\hat{\mathbf{x}}_{k|N}^{(e)}$ with covariances $\boldsymbol{\Sigma}_{k|N}^{(e)}$ and $\boldsymbol{\Sigma}_{k,k-1|N}^{(e)}$. The recursive equations of the algorithm are given e.g. in [24].

In order to take the expectation in (7), a linearisation of the state transition function $\mathbf{f}(\mathbf{x}_k)$ around $\hat{\mathbf{x}}_{k|N}^{(e)}$ is performed [16]. The Jacobian is denoted as $\mathbf{A}_k^{(e)} = \nabla_{\mathbf{x}} \mathbf{f}(\mathbf{x}_k)$. In contrast to numerical integration, e.g. [25], this yields a closed-form expression for $q_{\hat{\mathbf{Q}}_l}(\mathbf{Q})$ up to a constant:

$$q_{\hat{\mathbf{Q}}_l}(\mathbf{Q}) = -\frac{1}{2} N_{\text{seq}} (N-1) \log\det(\mathbf{Q}) - \frac{1}{2} \text{tr}\left(\mathbf{Q}^{-1}\mathbf{M}\right), \tag{9a}$$

$$\text{where } \mathbf{M} = \sum_{e=1}^{N_{\text{seq}}} \sum_{k=2}^{N} \mathbf{M}_k^{(e)},$$

$$\mathbf{M}_k^{(e)} = \begin{bmatrix} -\mathbf{A}_{k-1}^{(e)} & \mathbf{I}_{n\times n} \end{bmatrix} \begin{bmatrix} \boldsymbol{\Sigma}_{k-1|N}^{(e)} & \boldsymbol{\Sigma}_{k,k-1|N}^{(e)\top} \\ \boldsymbol{\Sigma}_{k,k-1|N}^{(e)} & \boldsymbol{\Sigma}_{k|N}^{(e)} \end{bmatrix} \begin{bmatrix} \cdot \end{bmatrix}^\top + \left(\hat{\mathbf{x}}_{k|N}^{(e)} - \mathbf{f}\left(\hat{\mathbf{x}}_{k-1|N}^{(e)}\right)\right)\left(\cdot\right)^\top . \tag{9b}$$

C. M-Step

The objective is now to maximise the scalar expected log-likelihood $q_{\hat{\mathbf{Q}}_l}(\mathbf{Q})$ from (9a) with respect to $\mathbf{Q}$. Employing matrix differentials [26], it follows that:

$$\frac{\partial}{\partial \mathbf{Q}} q_{\hat{\mathbf{Q}}_l}(\mathbf{Q}) = -\frac{1}{2} N_{\text{seq}} (N-1) \mathbf{Q}^{-1} + \frac{1}{2} \mathbf{Q}^{-1} \mathbf{M}^\top \mathbf{Q}^{-1} \ . \tag{10}$$

Thus, one obtains the result of the maximisation step [16]:

$$\hat{\mathbf{Q}}_{l+1} = \frac{1}{N_{\text{seq}}(N-1)} \mathbf{M}^\top \ . \tag{11}$$

Note that retrieving a point estimate only ignores valuable information that is contained in the data and likelihood function. Confidence (or standard error) intervals can be calculated to obtain a more informed view.

One approach to find such intervals is built on the asymptotic Gaussianity of maximum likelihood estimates, i.e. $\hat{\boldsymbol{\theta}} \sim \mathcal{N}\left(\boldsymbol{\theta}, \boldsymbol{\mathcal{I}}_{\mathbf{Y}}^{-1}(\boldsymbol{\theta})\right)$. The information matrix $\boldsymbol{\mathcal{I}}_{\mathbf{Y}}(\boldsymbol{\theta})$ is given by the negative Hessian of the log-likelihood:

$$\boldsymbol{\mathcal{I}}_{\mathbf{Y}}(\boldsymbol{\theta}) = -\mathbb{E}\left[\nabla_{\boldsymbol{\theta}} \nabla_{\boldsymbol{\theta}}^\top \log p(\mathbf{Y}|\boldsymbol{\theta})\right] \ . \tag{12}$$

Because the likelihood of the complete data is unavailable, the expected log-likelihood $q_{\hat{\boldsymbol{\theta}}_l}(\boldsymbol{\theta})$ at the time of convergence of the EM-algorithm is used instead [27]. Explicit expressions for the EM-algorithm are contained in [28].

D. Covariance matrix with Kronecker product structure

In the previous section, an estimate of the full $n \times n$ dimensional $\mathbf{Q}$ has been obtained. For the linear translational models from Sec. II-B though, this process noise covariance can be decomposed in a known part and an unknown, lower-dimensional one, i.e. the spectral density $\mathbf{S}$ of the continuous-time noise. For instance, the discretisation (3b) for the CV model with $\mathbf{S} = \text{diag}\left(\begin{bmatrix} S_x & S_y \end{bmatrix}\right)$ reads:

$$\begin{aligned} \mathbf{Q}(t_{k+1}, t_k) &= \begin{bmatrix} \frac{1}{3}T^3 S_x & \frac{1}{2}T^2 S_x & 0 & 0 \\ \frac{1}{2}T^2 S_x & T S_x & 0 & 0 \\ 0 & 0 & \frac{1}{3}T^3 S_y & \frac{1}{2}T^2 S_y \\ 0 & 0 & \frac{1}{2}T^2 S_y & T S_y \end{bmatrix} \\ &= \mathbf{S} \otimes \mathbf{Q}_1, \text{with } \mathbf{Q}_1 := \begin{bmatrix} \frac{1}{3}T^3 & \frac{1}{2}T^2 \\ \frac{1}{2}T^2 & T \end{bmatrix} \ . \end{aligned} \tag{13}$$

Exploiting that the $n_Q \times n_Q$ dimensional $\mathbf{Q}_1$ is known in order to solely estimate the $n_S \times n_S$ dimensional $\mathbf{S}$ has to the best of the authors' knowledge not been exemplified for the EM-algorithm. Related derivations exist though for covariance estimation of stationary time-series, e.g. [29], [30]. In the following, a generic closed-form solution to the

estimation of $\mathbf{S}$ will be derived, that is a modification of the M-Step from Sec. III-C.

At first, the relation (13) is inserted into (9a) and thus the expected log-likelihood $q_{\hat{\mathbf{S}}_l}(\mathbf{S})$ is obtained. Then, instead of (10), one has the following derivative with respect to $\mathbf{S}$:

$$\frac{\partial}{\partial \mathbf{S}} q_{\hat{\mathbf{S}}_l}(\mathbf{S}) = \tag{14}$$
$$-\frac{1}{2} N_{\mathrm{seq}} (N-1) n_Q \mathbf{S}^{-1} - \frac{1}{2} \frac{\partial}{\partial \mathbf{S}} \mathrm{tr}\left(\left(\mathbf{S}^{-1} \otimes \mathbf{Q}_1^{-1} \right) \mathbf{M} \right).$$

In order to solve for $\mathbf{S}$, (14) is reformulated. This is done using an abbreviation for the inverse of $\mathbf{Q}_1$, namely $\tilde{Q}_{ij} := \left[\mathbf{Q}_1^{-1}\right]_{ij}$. Moreover, we introduce the $n_S \times n_S$ matrix $\tilde{\mathbf{M}}^{(j,i)}$ whose elements are taken from $\mathbf{M}$ at a regular pattern:

$$\tilde{\mathbf{M}}^{(j,i)} = \left[M_{j+(u-1)n_Q,\ i+(v-1)n_Q} \right]_{\substack{u=1\ldots n_S \\ v=1\ldots n_S}}. \tag{15}$$

With these notations, one can write

$$\mathrm{tr}\left(\left(\mathbf{S}^{-1} \otimes \mathbf{Q}_1^{-1} \right) \mathbf{M} \right) = \sum_{i=1}^{n_Q} \sum_{j=1}^{n_Q} \tilde{Q}_{ij} \mathrm{tr}\left(\mathbf{S}^{-1} \tilde{\mathbf{M}}^{(j,i)} \right) \tag{16}$$

and after differentiation in (14) obtains the following estimate

$$\hat{\mathbf{S}}_{l+1} = \frac{1}{N_{\mathrm{seq}} (N-1) n_Q} \left(\sum_{i=1}^{n_Q} \sum_{j=1}^{n_Q} \tilde{Q}_{ij} \tilde{\mathbf{M}}^{(j,i)} \right)^{\top}. \tag{17}$$

IV. Application

A. Implementation of the EM-algorithm

Two aspects relevant for the implementation of the EM-algorithm will be briefly discussed. Firstly, each iteration of the E-Step includes a Kalman smoother run and hence computationally expensive matrix inversions. It is proposed in [31] to parallelise the E-Step and thus calculate $\mathbf{M}_k^{(e)}$ in (9b) independently for each sequence e.

Another suggestion leverages that for linear, time-invariant systems, the gain and covariance matrices converge to stationary values. These can therefore be pre-computed by numerically solving an algebraic Riccati equation [31].

An approach to reduce the number of iterations is to use an update rule with a better rate of convergence in the M-Step, e.g. a Newton-type scheme as described in [32].

Secondly, numerical robustness is concerned. Due to the iterative nature of the algorithm, round-off errors may accumulate. This can lead to negative definite estimates of a covariance matrix and divergence of the algorithm [23]. The numerical properties may be improved as follows:

- *E-Step:* A robust implementation of the Kalman smoother equations such as the square root form [23] can be used. Thus, it is ensured that the estimates $\mathbf{\Sigma}_k^{(e)}$, $\mathbf{\Sigma}_{k,k-1}^{(e)}$ are always positive definite.
- *M-Step:* The estimate of $\mathbf{Q}$ in (11) is based on the matrix $\mathbf{M}$. For notational convenience, the calculation of the individual $\mathbf{M}_k^{(e)}$ in (9b) is often explicitly written as additions and subtractions of matrices, e.g. [17], [31]. In order to avoid a potential loss of positivity due to round-off errors, [23] proposes an implementation based on Cholesky factorisations instead. Denote

$$\tilde{\mathbf{\Sigma}} = \mathrm{chol}\left(\begin{bmatrix} \mathbf{\Sigma}_{k-1|N}^{(e)} & \mathbf{\Sigma}_{k,k-1|N}^{(e)\top} \\ \mathbf{\Sigma}_{k,k-1|N}^{(e)} & \mathbf{\Sigma}_{k|N}^{(e)} \end{bmatrix} \right) \tag{18}$$

and $\mathbf{\Gamma}_k^{(e)} = \begin{bmatrix} -\mathbf{A}_{k-1}^{(e)} & \mathbf{I}_{n\times n} \end{bmatrix} \tilde{\mathbf{\Sigma}}^{\top}$, so that

$$\mathbf{M}_k^{(e)} = \mathbf{\Gamma}\mathbf{\Gamma}^{\top} + \left(\hat{\mathbf{x}}_{k|N}^{(e)} - \mathbf{f}\left(\hat{\mathbf{x}}_{k-1|N}^{(e)} \right) \right) \left(\cdot \right)^{\top} \tag{19}$$

is always positive definite.

B. Trajectory dataset and pre-processing

For the professed goal to determine the deviation between predictive models and recorded trajectories, two ways to acquire the necessary data can be taken into consideration.

The first is to equip the ego vehicle with recording devices with which the required CAN-signals can be captured. Advantages of this method are the low efforts concerning measuring instruments and the generation of precise data. The drawback is a lack of diversity in vehicles and driving styles as only one car and driver is recorded at a time.

Therefore, a second approach was favoured. Both the CAN-data of the ego vehicle and the positions and motions of objects in the vehicle's environment are measured. For the detection of the surrounding objects, the ego vehicle was additionally provided with a laser scanner. Hence, variations caused by different driving styles and vehicles are included in the dataset, which comprises $\approx 170\,\mathrm{h}$ of raw data. However, several preprocessing steps have to be performed on the exteroceptive measurements, which are explained in the following paragraphs.

a) Filtering: Detections which do not represent road users, like traffic signs or pedestrians, have to be filtered out of the measured objects. Employing the results of a classifier built-in the laser scanner, all recordings apart from cars, trucks and motorcycles are sorted out.

b) Transformation to ground-fixed coordinates: Using the recorded CAN-data for velocity, acceleration and yaw rate, the trajectories of the ego vehicle in a ground-fixed coordinate system can be calculated. Based on these, the trajectories of the remaining objects can be determined from the relative ranges between host and detected vehicles, which are measured by the laser sensor.

c) Classification of road user types: In the next processing step, vehicles are categorised into those driving on the same lane, in the same direction and parked or oncoming vehicles. For the sake of data precision, only vehicles driving on the same lane are regarded for the evaluation purposes. The motivation is that the subsequent manoeuvre classification task can be based on the ego vehicle CAN-data, because both the tracked vehicle and the following ego vehicle drive along the same route but at different times.

d) Classification of manoeuvres: For the purpose of an in-depth evaluation of the motion models, the recorded trajectories of vehicles driving on the same lane are analysed for certain frequently occurring manoeuvres (straight driving,

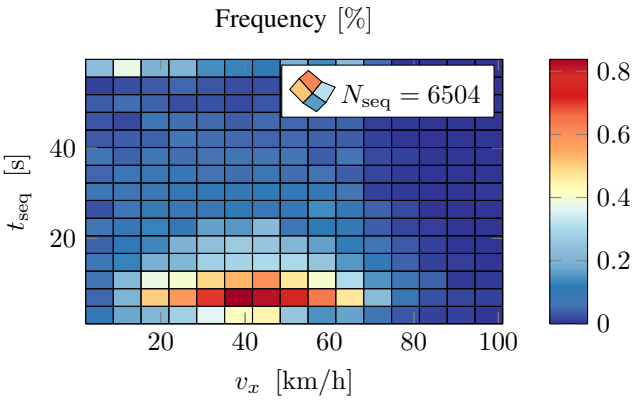

Fig. 3: Visualisation of mean absolute velocity and duration of straight driving episodes in the dataset.

TABLE II: Estimated parameter values

Model	Parameter estimates
CV	$S_x = \left(0.629\,\mathrm{m/s^2}\right)^2\,\mathrm{s}^{-1}$, $S_y = \left(0.472\,\mathrm{m/s^2}\right)^2\,\mathrm{s}^{-1}$
CA	$S_x = \left(0.511\,\mathrm{m/s^3}\right)^2\,\mathrm{s}^{-1}$, $S_y = \left(0.570\,\mathrm{m/s^3}\right)^2\,\mathrm{s}^{-1}$
CTRA	$S_a = \left(0.282\,\mathrm{m/s^3}\right)^2\,\mathrm{s}^{-1}$, $S_\omega = \left(1.6\,^\circ\mathrm{/s^2}\right)^2\,\mathrm{s}^{-1}$

curves or turning). Afterwards, the recordings are split at the transitions between the manoeuvres.

The reason for this is that manoeuvre changes severely violate the model's crucial assumptions. Hence, without further information about the driver's intention any of the considered models will fail to correctly predict a future change which is not indicated in the current state.

e) Distribution into sequences: As a final processing step the trajectories, which do now throughout represent one manoeuvre type, are collected. Thus, three datasets which contain episodes of straight driving, curves and turns are obtained. Fig. 3 visualises the duration and velocity distribution of the straight driving recordings. The overall dataset is furthermore separated in an evenly chosen portion (10%) for parameter estimation as well as the remaining 90% for evaluation purposes. Process noise parameters for the motion models from Tab. I are then estimated, with the eventual results shown in Tab. II.

For the CTRA model, further analyses on curved trajectories have been performed but are not shown here for brevity.

V. Evaluation

The goal of the following evaluation is twofold:

1) Is the assumption of Gaussian white process noise reasonable?
2) Are the obtained parameter values reasonable and generalise to other data than the ones used for estimation?

To address these questions, $N_{\text{seq,eval}} = 14437$ trajectory sequences of straight driving with a duration of 6 s each are first extracted from the evaluation dataset.

In order to calculate predictions with the three models from Sec. II-B, an initial state value is required. Henceforth, an Extended Kalman filter is applied to the first 3 s of each trajectory and an estimate $\left(\mathbf{x}\left(t_0\right), \mathbf{\Sigma}_{\mathbf{x}}\left(t_0\right)\right)$ obtained. The actual prediction $\mathbf{x}\left(t_0 + t_{\text{pred}}\right)$ is then calculated for the subsequent $t_{\text{pred}} = 0\,\mathrm{s} \ldots 3\,\mathrm{s}$, from (1). A covariance prediction $\mathbf{\Sigma}_{\mathbf{x}}\left(t_0 + t_{\text{pred}}\right)$ is derived according to (3).

Reference values for comparison are obtained by applying an Extended Kalman smoother to the overall recording. As the longitudinal motion is of main interest for straight trajectories, the longitudinal position and velocity errors $\Delta x\left(t_{\text{pred}}\right)$ and $\Delta v_x\left(t_{\text{pred}}\right)$ are used for evaluation.

By calculating the errors for each trajectory at each time step of the prediction horizon, empirical error distributions are obtained. These are compared to the normal distributions defined by the predicted covariances[2] $\mathbf{\Sigma}_{\mathbf{x}}\left(t_0 + t_{\text{pred}}\right)$.

The comparisons are visualised for three distinct times in terms of the histograms in Fig. 4a and quantile-quantile plots in Fig. 4b for position errors. Fig. 5 depicts the velocity errors. Moreover, 68% percentile values of the absolute errors over t_{pred} are displayed in Fig. 6 and compared to the corresponding 1σ-value of the predicted normal distribution.

As it is expected, the results exemplify how uncertainty increases with prediction time. Comparing the CV and CA model, slightly smaller errors are observed for the latter, which concurs with the findings in [6].

The histograms and quantile-quantile plots show a non-Gaussian error distribution. On the one hand, heavy tails are observed, i.e. high deviations occur more frequently than expected. This occurs for the CV and CTRA models in Fig. 4b. On the other hand, the distribution peaks are underestimated, most notable for the CA model as seen in Fig. 4a and Fig. 6.

In Fig. 6, deviations between the model predictions and the observed errors in terms of the 68% percentile are the smallest for the CV model and increase with prediction time.

Possible reasons for these deviations are a violation of the assumption of white, uncorrelated driver inputs which is a strong simplification of reality. If acceleration commands (not considered by the CV model) are applied, these will certainly last for time spans up to multiple seconds. A similar reasoning explains the overly represented peaks of the acceleration models, where a driver keeps his inputs at a constant value (i.e. correlated) for some time.

Despite the non-Gaussianity, a conclusion on the validity of the estimated process noise parameters is sought. To this end, a normal distribution is fitted to the error sample at each time step. This is the best possible description of the errors by a Gaussian distribution and thus a reference for the model that is estimated from the training dataset.

[2]In fact, slightly different variances are predicted for each sequence, depending on the initial Kalman filter estimate. Hence, the mean value is taken for the evaluation.

Overall, the reference fits are better adapted to the distribution peaks. Fig. 6 shows that the 68% percentile values are slightly overestimated as well, lying in between the data and model prediction. This indicates that the method was correctly applied and yields sensible estimates within the limits of the underlying model assumptions.

VI. Conclusion

A method for estimating process noise parameters of vehicle motion models from recorded trajectories has been proposed, applied to three commonly used models and evaluated. The results are Gaussian models which allow for closed-form uncertainty prediction. Despite certain disadvantages that come with this simple model structure, reasonable predictions are achieved. With the analytical expressions for uncertainty, algorithms for situation assessment can be enhanced for more informed decision making.

The expectation maximisation algorithm that is used for model identification has been thoroughly reviewed in terms of theoretical aspects and its practical implementation. A proposed novel contribution is a modified M-Step which takes into account the special structure of the process noise covariance in linear translational motion models.

For future works, enhancing the model structure to noise processes with time correlation or non-Gaussian amplitudes is an interesting objective. In order to maintain closed-form solutions, one can attempt to explicitly model the time correlation with an extended state vector for multiple time steps. The correlation coefficients and process noise parameters of the extended system model can then be estimated by the EM-algorithm [31]. Another approach is to assume a non-Gaussian distribution of the process noise amplitudes with heavier tails, e.g. a bimodal Gaussian mixture.

References

[1] M. Brännström, F. Sandblom, and L. Hammarstrand, "A probabilistic framework for decision-making in collision avoidance systems," *Intelligent Transportation Systems, IEEE Transactions on*, vol. 14, no. 2, pp. 637–648, 2013.

[2] J. E. Stellet, J. Schumacher, W. Branz, and J. M. Zöllner, "Uncertainty propagation in criticality measures for driver assistance," in *Intelligent Vehicles Symposium (IV), 2015 IEEE*, 2015.

[3] A. Kelly, "Linearized error propagation in odometry," *The International Journal of Robotics Research*, vol. 23, no. 2, pp. 179–218, 2004.

[4] X. Li and V. Jilkov, "Survey of maneuvering target tracking. part i. dynamic models," *Aerospace and Electronic Systems, IEEE Transactions on*, vol. 39, no. 4, pp. 1333–1364, 2003.

[5] X. Yuan, F. Lian, and C. Han, "Models and algorithms for tracking target with coordinated turn motion," *Mathematical Problems in Engineering*, pp. 1–10, 2014.

[6] R. Schubert, C. Adam, M. Obst, N. Mattern, V. Leonhardt, and G. Wanielik, "Empirical evaluation of vehicular models for ego motion estimation," in *Intelligent Vehicles Symposium (IV), 2011 IEEE*, pp. 534–539, 2011.

[7] A. Kapp, *Ein Beitrag zur Verbesserung und Erweiterung der Lidar-Signalverarbeitung für Fahrzeuge*. PhD thesis, Universität Karlsruhe (TH), Karlsruhe, 2007.

[8] N. Kämpchen, *Feature-Level Fusion of Laser Scanner and Video Data for Advanced Driver Assistance Systems*. PhD thesis, Universität Ulm, 2007.

[9] M. Lei, C. Han, and P. Liu, "Expectation maximization (em) algorithm-based nonlinear target tracking with adaptive state transition matrix and noise covariance," in *Information Fusion, 2007 10th International Conference on*, pp. 1–7, 2007.

[10] M. Bevermeier, S. Peschke, and R. Haeb-Umbach, "Joint parameter estimation and tracking in a multi-stage Kalman filter for vehicle positioning," in *Vehicular Technology Conference, 2009. VTC Spring 2009. IEEE 69th*, pp. 1–5, 2009.

[11] S. Lefèvre, D. Vasquez, and C. Laugier, "A survey on motion prediction and risk assessment for intelligent vehicles," *ROBOMECH Journal*, vol. 1, no. 1, 2014.

[12] J. Sörstedt, L. Svensson, F. Sandblom, and L. Hammarstrand, "A new vehicle motion model for improved predictions and situation assessment," *Intelligent Transportation Systems, IEEE Transactions on*, vol. 12, no. 4, pp. 1209–1219, 2011.

[13] J. Jansson, *Collision Avoidance Theory : with Application to Automotive Collision Mitigation*. PhD thesis, Linköping University, Department of Electrical Engineering, 2005.

[14] M. Schreier, V. Willert, and J. Adamy, "Bayesian, maneuver-based, long-term trajectory prediction and criticality assessment for driver assistance systems," in *Intelligent Transportation Systems (ITSC), 17th International IEEE Conference on*, pp. 334–341, 2014.

[15] A. P. Dempster, N. M. Laird, and D. B. Rubin, "Maximum likelihood from incomplete data via the em algorithm," *Journal Of The Royal Statistical Society, Series B.*, vol. 39, no. 1, pp. 1–38, 1977.

[16] P. Axelsson, U. Orguner, F. Gustafsson, and M. Norrlöf, "ML estimation of process noise variance in dynamic systems," in *Proceedings of the 18th IFAC World Congress*, pp. 5609–5614, 2011.

[17] C.-Y. Lin and M. Tomizuka, "Probabilistic approach to modeling and parameter learning of indirect drive robots from incomplete data," *Mechatronics, IEEE/ASME Transactions on*, vol. PP, no. 99, pp. 1–10, 2014.

[18] X. Ma and I. Andreasson, "Behavior measurement, analysis, and regime classification in car following," *Intelligent Transportation Systems, IEEE Transactions on*, vol. 8, no. 1, pp. 144–156, 2007.

[19] A. Gelb, ed., *Applied optimal estimation*. Cambridge, Mass.: M.I.T. Press, 1974.

[20] F. Gustafsson and A. Isaksson, "Best choice of coordinate system for tracking coordinated turns," in *Decision and Control, 1996., Proceedings of the 35th IEEE Conference on*, vol. 3, pp. 3145–3150 vol.3, 1996.

[21] M. Roth, G. Hendeby, and F. Gustafsson, "EKF/UKF maneuvering target tracking using coordinated turn models with polar/cartesian velocity," in *Information Fusion (FUSION), 2014 17th International Conference on*, pp. 1–8, 2014.

[22] J. Kooij, N. Schneider, and D. Gavrila, "Analysis of pedestrian dynamics from a vehicle perspective," in *Intelligent Vehicles Symposium Proceedings, 2014 IEEE*, pp. 1445–1450, 2014.

[23] S. Gibson and B. Ninness, "Robust maximum-likelihood estimation of multivariable dynamic systems," *Automatica*, vol. 41, no. 10, pp. 1667–1682, 2005.

[24] M. Y. Byron, K. V. Shenoy, and M. Sahani, "Derivation of extended Kalman filtering and smoothing equations," tech. rep., Stanford University, Department of Electrical Engineering, 2004.

[25] T. B. Schön, A. Wills, and B. Ninness, "System identification of nonlinear state-space models," *Automatica*, vol. 47, no. 1, pp. 39–49, 2011.

[26] J. R. Magnus, *Matrix differential calculus with applications in statistics and econometrics*. Wiley Series in Probability and Statistics, Chichester [u.a.]: John Wiley, rev. ed., repr. ed., 2002.

[27] R. H. Shumway, "Time series analysis and its applications : With r examples," 2011.

[28] L. Sommerlade, M. Thiel, M. Mader, W. Mader, J. Timmer, B. Platt, and B. Schelter, "Assessing the strength of directed influences among neural signals: An approach to noisy data," *Journal of Neuroscience Methods*, vol. 239, no. 0, pp. 47–64, 2015.

[29] N. Lu and D. L. Zimmermann, "On likelihood-based inference for a separable covariance matrix," tech. rep., University of Iowa, 2004.

[30] K. Werner, M. Jansson, and P. Stoica, "On estimation of covariance matrices with kronecker product structure," *Signal Processing, IEEE Transactions on*, vol. 56, no. 2, pp. 478–491, 2008.

[31] W. Mader, Y. Linke, M. Mader, L. Sommerlade, J. Timmer, and B. Schelterom, "A numerically efficient implementation of the expectation maximization algorithm for state space models," *Applied Mathematics and Computation*, vol. 241, no. 0, pp. 222–232, 2014.

[32] G. Goodwin and J. Aguero, "Approximate em algorithms for parameter and state estimation in nonlinear stochastic models," in *Decision and Control, 2005 and 2005 European Control Conference. CDC-ECC '05. 44th IEEE Conference on*, pp. 368–373, 2005.

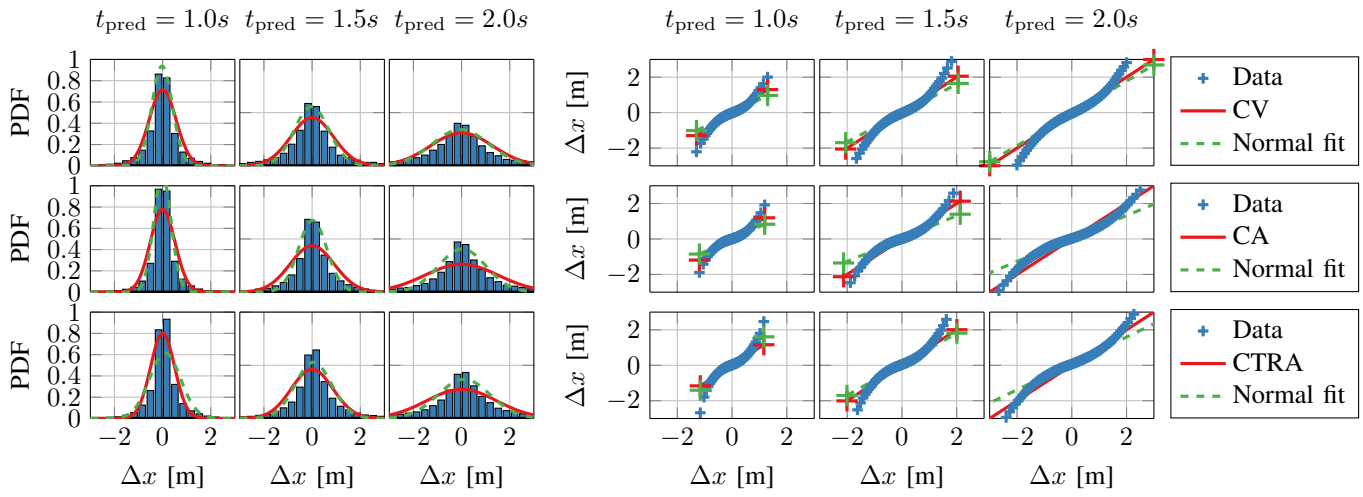

(a) Histograms

(b) Quantiles over model quantiles (range: $1\% \ldots 99\%$)

Fig. 4: Prediction errors in x for different prediction times $t_{\text{pred}} \in \{1\,\text{s}, 1.5\,\text{s}, 2\,\text{s}\}$ compared to the prediction model distributions and a-posteriori Gaussian fits. The non-Gaussianity of the error distribution becomes apparent in the non-linear shape of the quantile-quantile plots. Still, the a-posteriori fits that are used to validate the model agree with the predicted distribution in most cases. Hence, the derived model provides a reasonable prediction within the limits of a Gaussian model.

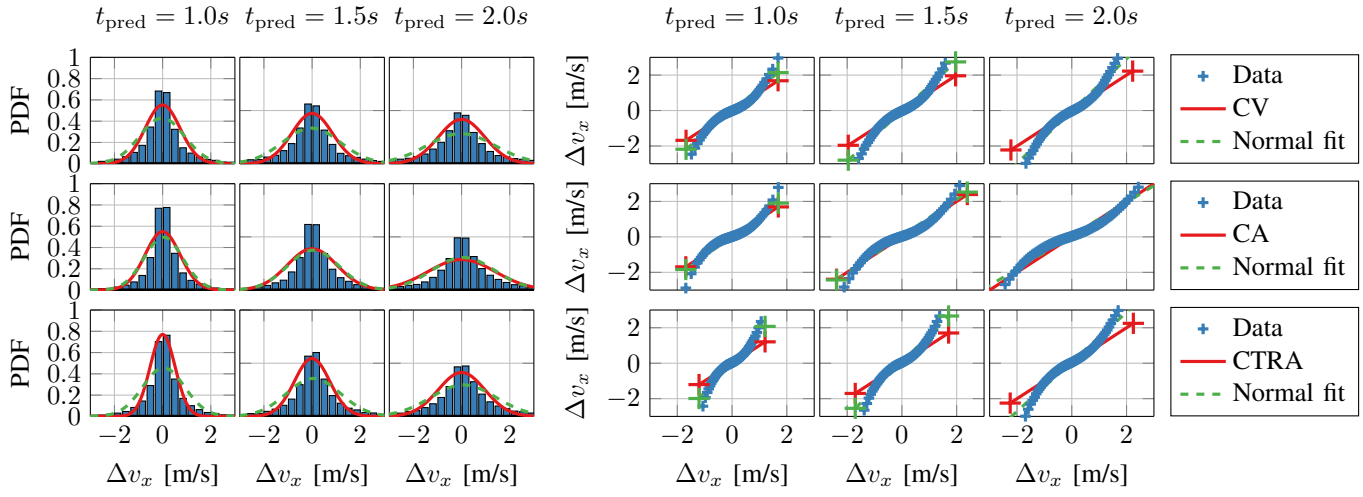

(a) Histograms

(b) Quantiles over model quantiles (range: $1\% \ldots 99\%$)

Fig. 5: Prediction errors in v_x for different prediction times $t_{\text{pred}} \in \{1\,\text{s}, 1.5\,\text{s}, 2\,\text{s}\}$ compared to the prediction model distributions and a-posteriori Gaussian fits.

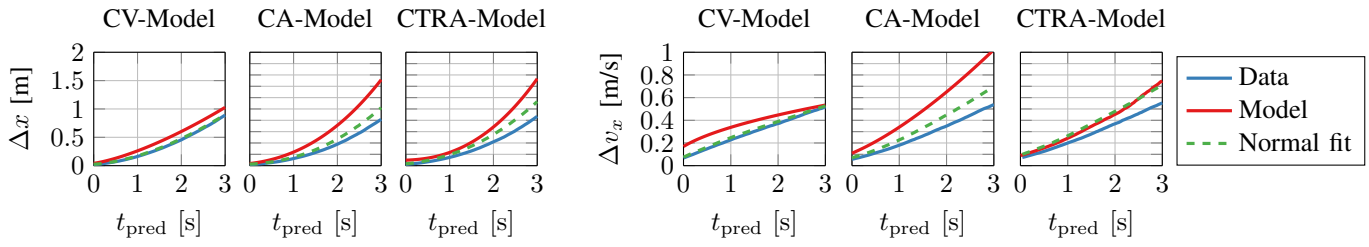

(a) Position x

(b) Velocity v_x

Fig. 6: 68% percentile values of observed errors, model predictions and a-posteriori normal fits. Increasing deviations are observed at higher prediction horizon. For the CA model, the data shows an overly strong peak around the mean (as seen in Fig. 4a) which is not captured and hence the predicted percentile values are too conservative. For velocity errors in the CV model, a qualitative deviation from the theoretical evolution $\sigma_{\Delta v_x}(t_{\text{pred}}) \propto \sqrt{t_{\text{pred}}}$ can be observed.